NDT-CE 2022 - The International Symposium
on Nondestructive Testing in Civil Engineering
Zurich, Switzerland, August 16-18, 2022

OsciCheck: A Novel Fluidic Transducer for Air-Coupled Ultrasonic Measurements

Benjamin BÜHLING[1]*, Stefan MAACK[1], Christoph STRANGFELD[1]

[1] Department 8: "Non-destructive Testing", Federal Institute for Materials Research and Testing (BAM); Berlin, Germany
*Corresponding author, e-mail address: benjamin.buehling@bam.de

Abstract
Ultrasonic measurement technology has become indispensable in NDT-CE. Air-coupled ultrasonic (ACU) measurement techniques promise to reduce measurement time. However, the signal quality suffers from large specific impedance mismatch at the transducer-air and air-specimen interface. Additionally, large pressure amplitudes are necessary for the penetration depth required in NDT-CE applications.
To address the specific requirements of ultrasonic testing in NDT-CE, a robust ACU transducer was developed, that generates ultrasound by quickly switching a pressurized air flow. The simple design of the fluidic transducer makes the device maintenance free and resilient against harsh environmental conditions. Since the signal is generated by aeroacoustics, there is no specific impedance mismatch between the transducer and the surrounding air. The ultrasonic signal exhibits frequencies in the 30-60 kHz range and is therefore well suited to penetrate heterogenous materials such as concrete. This contribution gives an introduction in the working principle and signal characteristics of the fluidic transducer. Its applicability to measurements in concrete is verified. A detailed outlook is given to discuss the future potential of fluidic ultrasonic actuators.
Keywords: air-coupled ultrasound, nondestructive testing, fluidics, bistable amplifier, aeroacoustics

1 Introduction

Ultrasonic testing is a common measurement technique in nondestructive testing of materials [1], including applications in civil engineering (NDT-CE) [2]. Due to broad variety of material and structural properties encountered in NDT-CE, various restrictions exist concerning the choice of wave properties used for the measurements. Concrete, the most widely used building material [3, 4], has a heterogeneous structure that consists of its cement matrix as well as aggregates and pores [5]. These heterogeneities cause scattering of acoustic waves that are coupled into the specimen, which increases with decreasing wavelength of the ultrasonic signal [6]. In order to retain a sufficient signal-to-noise ratio (SNR) for time-of-flight (TOF) measurements, the frequency of the signal applied in NDT-CE applications is limited to the lower ultrasonic range, commonly between 20 kHz and 150 kHz [7]. In this range, the wavelength is usually smaller than the dimensions of the specimen but larger than the inhomogeneities. Typical tasks in which ultrasonic testing is applied consider macro-scale properties of a specimen (e. g. thickness determination and detection of reinforcements or faults) or nano-scale properties of the material (e. g. the elasticity or water content) [8, 9]. When these tests are conducted at an existing structure, the travel path of the wave can be in the range of tens of centimeters up to several meters [8]. In addition to limiting the applicable wave types to bulk waves in many cases [2], the large dimensions of the specimens require the insertion of large acoustic amplitudes to compensate for attenuation due to scatter and absorption [6, 10]. The current state-of-the-art of ultrasonic testing is the use of dry point contact transducers that are pressed onto the specimen surface and can generate either longitudinal or shear waves into the specimen [2]. Using this approach, a considerable amount of the total measurement time is consumed by the relocation of the transducer head for each measurement point.

The use of air-coupled ultrasound (ACU) for ultrasonic testing is considered as a strategy to speed up measurements. However, the adoption of ACU is still restricted due to several challenges involved, one of them is the low amount of acoustic pressure entering the specimen. In ACU, the signal is generated by a transducer that is not in direct contact with the specimen but separated by an air gap. This intermediate layer of air has a strong impact on the acoustic pressure transmitted from the transducer to the specimen. Due to the large difference of specific acoustic impedances the transmission coefficient amounts to only -37.5 dB at the air-specimen interface [11] and -11.2 dB to -17.5 dB at the transducer-air interface [11, 12] of piezoelectric transducers. While the losses at the specimen interface are inevitable due to the measurement setup, the transducer interface offers potential to reduce the acoustic pressure losses and thus provides the signal amplitudes required in NDT-CE.

As part of the OsciCheck project at the Federal Institute for Materials Research and Testing (BAM), a novel transducer was developed that uses aeroacoustic mechanisms to generate an ultrasonic signal. The principal concept of this approach is to use aerodynamic instabilities instead of vibrating solids to generate sound. As a result, differences in specific acoustic impedance at the transducer-air interface are omitted to enable higher sound pressures entering the specimen. This contribution presents the working principle and signal properties of the fluidic transducer as well as suggestions on possible future applications.

2 Fluidic Transducer

Fluidics, a combination of the words *fluid* and *logic*, is a field of technology that is concerned with use of “fluid interactions to perform functions of sensing, logic, amplification, signal transmission, signal conditioning and control” [13], largely without the use of moving parts. At the time of its emergence in 1959, it was envisioned as an alternative to electronics and was developed rapidly in the 1960s and 1970s [14]. As it became clearer that fluidics could not keep pace with electronics development, it was largely abandoned [15]. Today, its main developments concern flow control for aerodynamic applications [16-18]. Nonetheless, the advantages of fluidic technology that drove their development in the past remain valid: Since the functions of fluidic devices are driven by fluid flow within static solid boundaries without electronics, they are virtually maintenance free, robust against shock and vibration, and operable in harsh environments, including those with extreme temperatures or radioactivity [14]. This robustness makes fluidics a promising platform for applications in NDT-CE.

2.1 Working Principle

The fluidic transducer is based on a bistable fluidic amplifier developed by Bobusch [19]. Figure 1a-d show the working principle of this basic fluidic device. If a pressurized fluid flow – air in our case – is attached to the supply port (S) of a bistable amplifier, the flow attaches to one of the side walls and exits through one of the two outlet ports (O1 and O2). The initial state of the device, i.e. the initially active outlet, can be forced by applying additional pressurized air to one of the control ports (C1 and C2), in Figure 1a it is C2. Due to the Coandă effect, the main flow stays attached to the side wall and continues to exit through the outlet port, even if the control flow is turned off (Fig. 1b). When pressurized air is applied to the opposite control port (C1 in Fig. 1c), the main flow switches rapidly from O2 to O1, attaches to the opposite side wall of the device and again reaches a stable state (Fig. 1d).

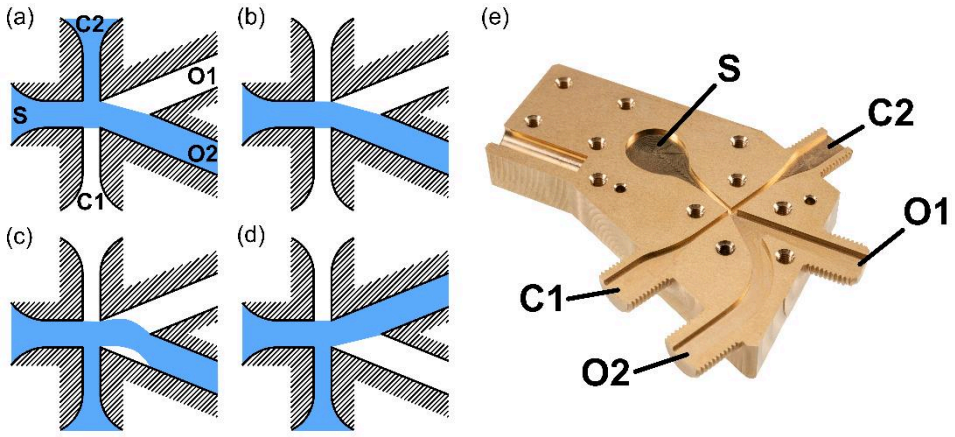

Figure 1: (a)-(d) Switching process of a bistable fluidic amplifier. Adapted from Ref. [20]. (e) Internal geometry of the fluidic transducer. S – supply port, C1 – control port 1, C2 – control port 2, O1 – outlet 1, O1 – outlet 2. Adapted from Ref. [21].

It is during this switching process that an ultrasonic pulse is generated and leaves the device through the outlet ports. This pulse is then followed by an air jet of near-sonic velocity, exiting the device [20, 22]. Figure 1e shows internal channels of the fluidic ultrasonic transducer, which are closed using a cover plate. The air enters S through the cover plate, while the control and outlet ports are threaded to attach connectors. In fluidic transducer operation, the stable flow states are defined as *on* and *off*, when the flow is exiting through O1 or O2, respectively. To reduce flow noise during *off* state, a silencer is attached to O2. For improved radiation impedance matching and enhancement of directivity of the pulse generated while switching *on*, an exponential horn is attached to O1 [23]. As a side effect, the horn acts as a diffuser for the air flow, so that its velocity is reduced and with it the risk of damaging the surface in case of soft materials instead of concrete, which otherwise could only be achieved by separating the propagation directions of flow and sound [24]. While S is supplied with constant pressurized air, C1 and C2 are controlled using solenoid valves, as outlined in Ref. [25].

2.2 Signal

Figure 2a shows a typical signal generated by the fluidic transducer with an attached exponential horn during a switching cycle in time domain. These data were acquired using a calibrated microphone (MK301, Microtech Gefell, Germany) on the acoustic axis of the transducer, 50 mm from it's the horn mouth. The waveform starts with low amplitude flow noise in the steady *off* state (ref. Fig. 1b). As the transducer switches *on* (ref. Fig. 1c), a strong acoustic pulse is generated, followed by a time interval of higher amplitude flow noise in the stable *on* state (ref. Fig. 1d). When switching *off* again, a secondary pulse is emitted, before the flow settles again at steady *off* state. In frequency domain (Fig. 2b), the about 2 ms interval of switching *on*, features three distinct ultrasound peaks at 30 kHz, 43 kHz, and 57 kHz. These values are averages of 40 recorded pulses, while each has slightly varying frequency content due to their origin in turbulent flow [21].

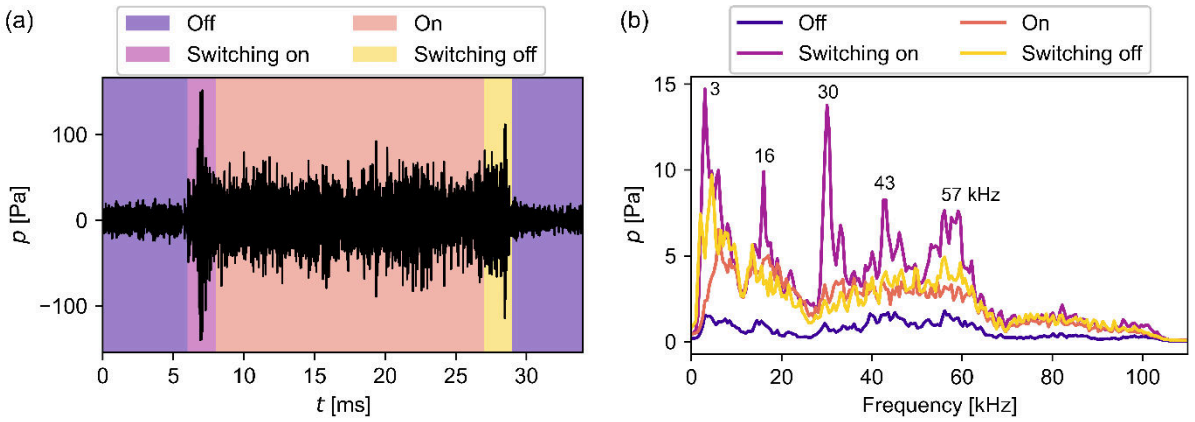

Figure 2: (a) Exemplary time signal of a fluidic transducer pulse with the switching process highlighted. (b) Averaged spectra during the various stages of the switching process.

3 Transmission Measurements

The applicability of the fluidic transducer for ultrasonic measurements was assessed at a stepped concrete test specimen featuring thicknesses of ranging from 80 mm to 240 mm in 40 mm steps (Fig. 3a). To enable fully non-contact TOF measurements, a novel all-optical measurement technique [26] was used, that is sketched in Figure 3b. In this method, two laser Doppler vibrometers (LDV) are used. The first LDV is placed between transducer and specimen, perpendicular to the specimen surface, and is operated in refracto-vibrometry (RV) mode [27, 28]. The second LDV is pointed at the back of the specimen and records the particle velocity at the specimen back surface caused by the transmitted ultrasonic pulse. When an acoustic signal is emitted by the transducer, it passes through the beam of the LDV in RV mode before reaching the specimen surface. A large portion of the signal is reflected due to the impedance mismatch at the interface and a smaller portion enters the specimen. The reflected portion of the signal then passes through the same beam again, allowing to find the exact time of arrival (TOA) at the specimen surface via autocorrelation. By cross-correlating the signals of both LDVs and correcting for this TOA, the TOF of the signal through the specimen is found. In addition to being fully contact-free, this method avoids impedance losses of the signal exiting the back surface of the specimen as the second LDV is measuring directly at that surface.

The resulting TOF and corresponding longitudinal sound velocities for the different thicknesses of the test specimen are shown in Figure 3c. The fluidic ACU results are compared to transmission measurements conducted using a 100 kHz longitudinal piezoelectric contact transducers (S0208, ACS, Russia) that were coupled to the specimen using petroleum jelly. At every measurement point, the air-coupled TOF is higher than the contact TOF, resulting in lower calculated sound velocity c_L. The largest difference is found at the thinnest part of the specimen, where the TOF difference is $\epsilon_t = 4.45$ µs, which corresponds to a sound velocity difference of

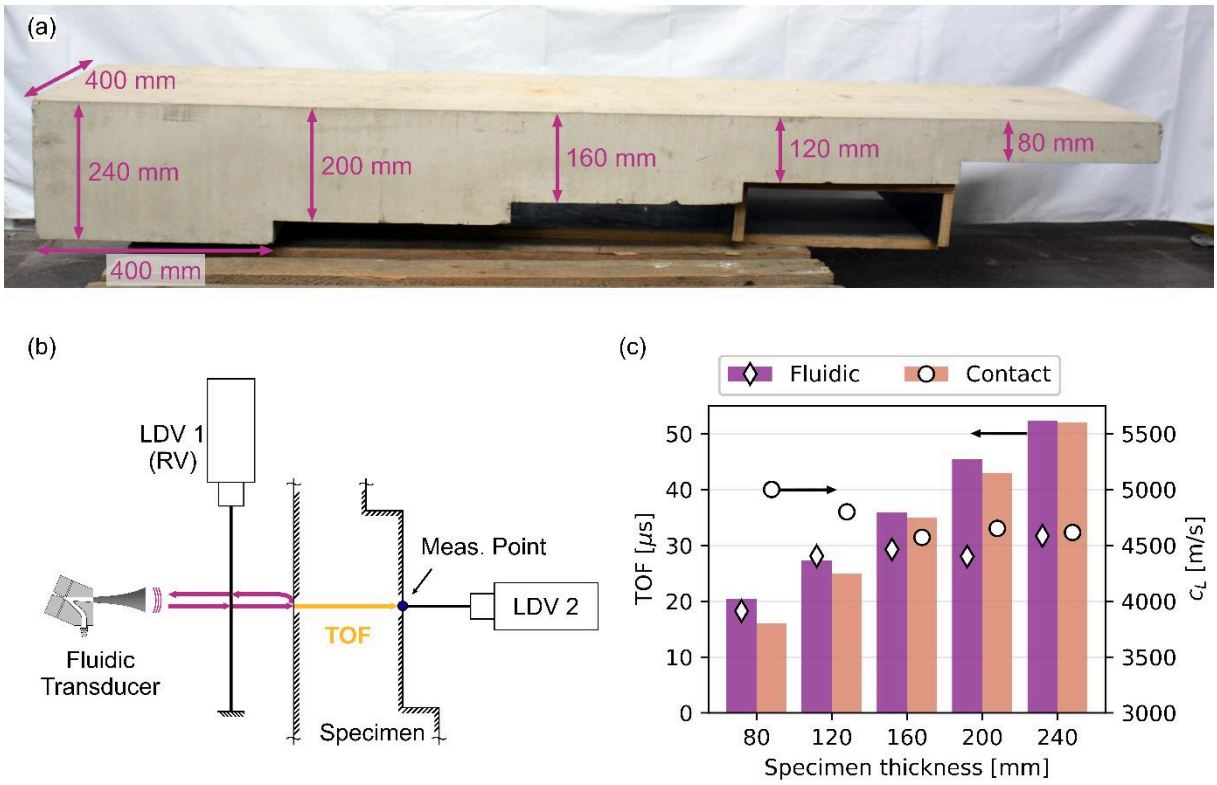

Figure 3: (a) Concrete specimen. (b) Fully non-contact measurement setup. The purple arrows indicate the in-air sound path, the yellow arrow indicates the path through the specimen. (c) Comparison of fluidic and contact results. Bars indicate the TOF, symbols indicate the corresponding calculated longitudinal propagation velocity c_L.

$\epsilon_c = 22$ %. As the specimen thickness increases, these differences decrease to $\epsilon_t = 0.35$ µs and $\epsilon_c = 0.7$ %.

4 Discussion and Outlook

The results presented in Figure 3c indicate a good agreement between the measurement results from the fluidic and contact transducer for larger concrete thicknesses, despite having minor deviations. Several factors may cause these differences. When comparing contact and air-coupled TOFs in concrete, the latter have been found higher by Purnell et al. [29] and Berriman et al. [30]. The authors attribute this behavior to a tendency of the air-coupled sound wave to couple into the lower impedance cement matrix instead of the aggregates. Additionally, the fluidic transducer signal has lower characteristic frequencies than the contact transducer. Given the dispersion in concrete [9], the lower frequency waves also have a lower propagation velocity. One reason for the large deviations at the thinnest part of the specimen may be the the wavelength of the contained frequencies of the fluidic pulse in concrete, that in this case are equal or even slightly longer than the specimen thickness.

These presented results indicate that the fluidic transducer is suitable as signal generator for ACU measurements in NDT-CE. It generates an air-coupled signal in the lower ultrasonic range relevant to NDT-CE that has sufficient acoustic pressure to penetrate at least 240 mm of concrete while not requiring a high voltage power supply and being robust against harsh

environments that may be encountered in practical measurements. However, the latter is not true for equipment required for receiving the data. Albeit allowing highly accurate measurements, LDVs are sensitive to vibrations and dusty environments, expensive and unhandy. This may restrict the application of the current setup to controlled laboratory environments. Future research toward improvement of the fluidic ultrasonic transducer, based on a fluidic amplifier, should include:

- The development of alternative measurement setups, that are more robust and may be able to be sensitive enough to sense in-air signals after transmission. These might include optical microphones [31] or even microphone arrays [32].
- Development of a deeper understanding on the sound generation mechanisms inside the transducer to decrease pulse length and vary spectral properties. Initial research has already been conducted [22]. However, the sensitivity of fluidic amplifiers to every change in geometry [33] paired with supersonic flow opens a wide parameters space for remarkable optimization.
- Application of the fluidic transducer in other domains than civil engineering, that feature harsh environments such as high temperatures or radiation [34, 35].

Beyond improvements concerning transducers based on the fluidic amplifier, also fluidic oscillators could be used as a source of sound generation. This device largely works like a bistable fluidic amplifier, but instead of actively triggering the control ports, self-sustained fluid instabilities control the switching [36]. Given constant fluid properties, the resulting flow oscillation depends only on the mass flow through the device. This behavior enables the generation of chirped signals by applying a mass flow ramp to the oscillator [37]. Using the resulting sound for NDT applications has been proposed [37, 38] and is planned to be implemented. Preliminary experiments conducted at BAM indicate that simply scaling down the geometry presented in [37, 38] increases the output frequency to the ultrasonic range, in accordance with theoretical models [39]. However, the frequency increase comes with a strongly reduced pressure amplitude due to a downscaled mass flow through the device, so that geometry improvements are necessary.

Acknowledgements

This research was funded by the German Federal Ministry for Economic Affairs and Climate Action (BMWK) under the ZIM (Zentrales Innovationsprogramm Mittelstand) grant ZF4044222WM7.

References

1. Krautkrämer, J. and H. Krautkrämer, *Ultrasonic Testing of Materials*. 4 ed, ed. J. Krautkrämer and H. Krautkrämer. 1990, Berlin, Heidelberg: Springer Berlin Heidelberg. DOI: 10.1007/978-3-662-10680-8.
2. Schickert, M. and M. Krause, *Ultrasonic techniques for evaluation of reinforced concrete structures*, in *Non-Destructive Evaluation of Reinforced Concrete Structures*, C. Maierhofer, H.-W. Reinhardt, and G. Dobmann, Editors. 2010, Woodhead

Publishing: Oxford, Cambridge, New Delhi. p. 490-530. DOI: 10.1533/9781845699604.2.490.
3. Huang, B., et al., *A Life Cycle Thinking Framework to Mitigate the Environmental Impact of Building Materials.* One Earth, 2020. **3**(5): p. 564-573. DOI: 10.1016/j.oneear.2020.10.010.
4. Abergel, T., et al., *2018 Global Status Report: Towards a zero-emission, efficient, and resilient buildings and construction sector*. 2018, United Nations Environment Programme: Nairobi, Kenya. p. 1-71. URL: https://www.worldgbc.org/news-media/2018-global-status-report-towards-zero-emission-efficient-and-resilient-buildings-and.
5. Saenger, E.H., *Time reverse characterization of sources in heterogeneous media.* NDT & E International, 2011. **44**(8): p. 751-759. DOI: 10.1016/j.ndteint.2011.07.011.
6. Asadollahi, A. and L. Khazanovich, *Numerical investigation of the effect of heterogeneity on the attenuation of shear waves in concrete.* Ultrasonics, 2019. **91**: p. 34-44. DOI: 10.1016/j.ultras.2018.07.011.
7. Planès, T. and E. Larose, *A review of ultrasonic Coda Wave Interferometry in concrete.* Cement and Concrete Research, 2013. **53**: p. 248-255. DOI: 10.1016/j.cemconres.2013.07.009.
8. Wiggenhauser, H. and H. Azari, *Classification of Nondestructive Evaluation Tasks for Reinforced Concrete Structures.* Journal of Infrastructure Systems, 2017. **23**(4): p. 04017021. DOI: 10.1061/(ASCE)IS.1943-555X.0000378.
9. Philippidis, T.P. and D.G. Aggelis, *Experimental study of wave dispersion and attenuation in concrete.* Ultrasonics, 2005. **43**(7): p. 584-595. DOI: 10.1016/j.ultras.2004.12.001.
10. Krautkrämer, J. and H. Krautkrämer, *Attenuation of Ultrasonic Waves in Solids*, in *Ultrasonic Testing of Materials*, J. Krautkrämer and H. Krautkrämer, Editors. 1990, Springer Berlin Heidelberg: Berlin, Heidelberg. p. 108-116. DOI: 10.1007/978-3-662-10680-8_7.
11. Gräfe, B., *Luftgekoppeltes Ultraschallecho-Verfahren für Betonbauteile*, in *Fakultät VI - Planen Bauen Umwelt*. 2009, Technische Universität Berlin: Berlin. DOI: 10.14279/depositonce-1964.
12. Kazys, J.R., R. Sliteris, and J. Sestoke, *Air-Coupled Low Frequency Ultrasonic Transducers and Arrays with PMN-32%PT Piezoelectric Crystals.* Sensors, 2017. **17**(1). DOI: 10.3390/s17010095.
13. SAE, A.A.F. Control, and C. Vehicle Management Systems, *ARP993D Fluidic Technology*. 2012-05, SAE International. DOI: 10.4271/ARP993D.
14. Joyce, J.W., *Fluidics: Basic Components and Applications*. 1983, Harry Diamond Laboratories: Adelphi, MD, USA. URL: https://apps.dtic.mil/sti/citations/ADA134046.
15. Tesař, V. *FLUIDICS: WHAT IT IS, WHERE IT IS HEADING - AND HOW IT WILL CHANGE THE WORLD WE LINE IN*. in *19th International Conference of Engineering Mechanics*. 2013. Svratka, Czech Republic: Institute of Thermomechanics, Academy of Sciences of the Czech Republic. URL: https://www.engmech.cz/im/proceedings/show_p/2013/3.
16. Wieser, D., et al., *Manipulation of the Aerodynamic Behavior of the DrivAer Model with Fluidic Oscillators.* SAE International Journal of Passenger Cars - Mechanical Systems, 2015. **8**(2): p. 687-702. DOI: 10.4271/2015-01-1540.

17. Tewes, P. and L. Taubert, *Control of Separation on a Swept Wing using Fluidic Oscillators*, in *53rd AIAA Aerospace Sciences Meeting*. DOI: 10.2514/6.2015-0783.
18. Cerretelli, C., et al., *Unsteady Separation Control for Wind Turbine Applications at Full Scale Reynolds Number*, in *47th AIAA Aerospace Sciences Meeting including The New Horizons Forum and Aerospace Exposition*. DOI: 10.2514/6.2009-380.
19. Bobusch, B.C., *Fluidic devices for realizing the shockless explosion combustion process*, in *Fakultät V - Verkehrs- und Maschinensysteme*. 2015, Technische Universität Berlin: Berlin. DOI: 10.14279/depositonce-4351.
20. Bühling, B., et al., *Experimental analysis of the acoustic field of an ultrasonic pulse induced by a fluidic switch.* The Journal of the Acoustical Society of America, 2021. **149**(4): p. 2150-2158. DOI: 10.1121/10.0003937.
21. Bühling, B., et al., *Enhancing the spectral signatures of ultrasonic fluidic transducer pulses for improved time-of-flight measurements.* Ultrasonics, 2022. **119**: p. 106612. DOI: 10.1016/j.ultras.2021.106612.
22. Schweitzer, T., et al., *Switching Action of a Bistable Fluidic Amplifier for Ultrasonic Testing.* Fluids, 2021. **6**(5): p. 171. DOI: 10.3390/fluids6050171.
23. Beranek, L.L. and T.J. Mellow, *Horn loudspeakers*, in *Acoustics: Sound Fields and Transducers*, L.L. Beranek and T.J. Mellow, Editors. 2012, Academic Press. p. 407-448. DOI: 10.1016/B978-0-12-391421-7.00009-9.
24. Bühling, B., S. Maack, and C. Strangfeld, *Using sonic crystals to separate the acoustic from the flow field of a fluidic transducer.* Applied Acoustics, 2022. **189**: p. 108608. DOI: 10.1016/j.apacoust.2021.108608.
25. Bühling, B., et al. *Influence of Operating Conditions on the Fluidic Ultrasonic Transducer Signal*. in *DAGA 2021*. 2021. Vienna, Austria: Deutsche Gesellschaft für Akustik e.V. (DEGA). URL: https://opus4.kobv.de/opus4-bam/frontdoor/index/index/docId/53493.
26. Bühling, B., et al., *Development of an Accurate and Robust Air-Coupled Ultrasonic Time-of-Flight Measurement Technique.* Sensors, 2022. **22**(6): p. 2135. DOI: 10.3390/s22062135.
27. Zipser, L. and H. Franke. *Visualization and measurement of acoustic and fluidic phenomena using a laser-scanning vibrometer*. in *Proc. SPIE*. 2002. SPIE. DOI: 10.1117/12.468183.
28. Torras-Rosell, A., S. Barrera-Figueroa, and F. Jacobsen, *Sound field reconstruction using acousto-optic tomography.* The Journal of the Acoustical Society of America, 2012. **131**(5): p. 3786-3793. DOI: 10.1121/1.3695394.
29. Purnell, P., et al., *Noncontact ultrasonic diagnostics in concrete: A preliminary investigation.* Cement and Concrete Research, 2004. **34**(7): p. 1185-1188. DOI: 10.1016/j.cemconres.2003.12.012.
30. Berriman, J., et al., *Humidity and aggregate content correction factors for air-coupled ultrasonic evaluation of concrete.* Ultrasonics, 2005. **43**(4): p. 211-217. DOI: 10.1016/j.ultras.2004.07.003.
31. Rus, J., et al., *Qualitative comparison of non-destructive methods for inspection of carbon fiber-reinforced polymer laminates.* Journal of Composite Materials, 2020. **54**(27): p. 4325-4337. DOI: 10.1177/0021998320931162.

32. Movahed, A., T. Waschkies, and U. Rabe, *Air Ultrasonic Signal Localization with a Beamforming Microphone Array.* Advances in Acoustics and Vibration, 2019. **2019**: p. 7691645. DOI: 10.1155/2019/7691645.
33. Warren, R.W., *Some parameters affecting the design of bistable fluid amplifiers*, in *Fluid jet control devices: papers presented at the winter annual meeting of the ASME*, F.T. Brown, Editor. 1962, American Society of Mechanical Engineers: New York. p. 75-82. URL: https://books.google.de/books/about/Symposium_on_Fluid_Jet_Control_Devices_a.html?id=b1BdjwEACAAJ&redir_esc=y.
34. Kazys, R. and V. Vaskeliene, *High Temperature Ultrasonic Transducers: A Review.* Sensors, 2021. **21**(9): p. 3200. DOI: 10.3390/s21093200.
35. Tittmann, B.R., et al., *State-of-the-Art and Practical Guide to Ultrasonic Transducers for Harsh Environments Including Temperatures above 2120 °F (1000 °C) and Neutron Flux above 1013 n/cm2.* Sensors, 2019. **19**(21). DOI: 10.3390/s19214755.
36. Bobusch, B.C., et al., *Experimental study of the internal flow structures inside a fluidic oscillator.* Experiments in Fluids, 2013. **54**(6): p. 1-12. DOI: 10.1007/s00348-013-1559-6.
37. Strangfeld, C., et al., *Frequency modulated, air-coupled ultrasound generated by fluidic oscillators.* (submitted).
38. Bühling, B., C. Strangfeld, and S. Maack. *Entwicklung eines luftgekoppelten Ultraschall-Echo-Prüfverfahrens mittels fluidischer Anregung*. in *DACH-Jahrestagung 2019*. 2019. Friedrichshafen, Germany: DGZfP Deutsche Gesellschaft für Zerstörungsfreie Prüfung. URL: https://opus4.kobv.de/opus4-bam/frontdoor/index/index/docId/48120.
39. Ghanami, S. and M. Farhadi, *Fluidic Oscillators' Applications, Structures and Mechanisms – A Review.* Challenges in Nano and Micro Scale Science and Technology, 2019. **7**(1): p. 9-27. DOI: 10.22111/tpnms.2018.25051.1153.